# MinION-based DNA barcoding of preserved and non-invasively collected wildlife samples

**Running title: MinION DNA barcoding of wildlife samples**

Adeline Seah[1,*], Marisa C.W. Lim[1,*], Denise McAloose[1], Stefan Prost[2,3], Tracie Seimon[1]

[1]Wildlife Conservation Society, Zoological Health Program, Bronx Zoo, 2300 Southern Blvd, Bronx, NY, 10460, USA
[2]LOEWE-Centre for Translational Biodiversity Genomics, Senckenberg Nature Research Society, Frankfurt, Germany
[3]South African National Biodiversity Institute, National Zoological Garden, Pretoria, South Africa
*Authors contributed equally

Corresponding author:
Marisa C.W. Lim
Wildlife Conservation Society
Zoological Health Program, Bronx Zoo
2300 Southern Blvd
Bronx Zoo, NY 10460, USA
mclim@wcs.org

## Abstract

1. The ability to sequence a variety of wildlife samples with portable, field-friendly equipment will have significant impacts on wildlife conservation and health applications. However, the only currently available field-friendly DNA sequencer, the MinION by Oxford Nanopore Technologies, has a high error rate compared to standard laboratory-based sequencing platforms and has not been systematically validated for DNA barcoding accuracy for preserved and non-invasively collected tissue samples.

2. We tested whether various wildlife sample types, field-friendly methods, and our clustering-based bioinformatics pipeline, SAIGA, can be used to generate consistent and accurate consensus sequences for species identification. Here, we systematically evaluate variation in cytochrome b sequences amplified from scat, hair, feather, fresh frozen liver, and formalin-fixed paraffin-embedded (FFPE) liver. Each sample was processed by three DNA extraction protocols.

3. For all sample types tested, the MinION consensus sequences matched the Sanger references with 99.29-100% sequence similarity, even for samples that were difficult to amplify, such as scat and FFPE tissue extracted with Chelex resin. Sequencing errors occurred primarily in homopolymer regions, as identified in previous MinION studies.

4. We demonstrate that it is possible to generate accurate DNA barcode sequences from preserved and non-invasively collected wildlife samples using portable MinION sequencing, creating more opportunities to apply portable sequencing technology for species identification.

**Keywords:** bioinformatics, conservation, laboratory methods, sequence data

## Introduction

Wildlife health and conservation initiatives benefit tremendously from genetic methods of species identification for infectious disease screening (Schlaberg, Chiu, Miller, Procop, & Weinstock, 2017; Gardy & Loman, 2018), detecting illegally traded wildlife products (Hobbs, Potts, Walsh, Usher, & Griffiths, 2019), uncovering food label fraud (Pardo et al., 2018; Galimberti et al., 2019; Hobbs et al., 2019), and documenting understudied biodiversity (Costa & Carvalho, 2007). One major challenge for wildlife molecular studies is obtaining fresh samples from live or dead wild animals. Such endeavors can be logistically challenging, generally involving highly skilled teams, detailed planning, and acquisition of permissions from local, regional and international partners and governmental agencies for animal handling, sample collection, and sample transfer for molecular testing. Consequently, environmental samples (Ficetola, Miaud, Pompanon, & Taberlet, 2008; Thomas et al., 2019) and animal samples that can be collected non-invasively (e.g. hair, feathers, scat, etc.) (Marshall & Ritland, 2002; Waits

58 & Paetkau, 2005; De Barba et al., 2014) are increasingly being used for ecological studies,
59 wildlife health assessments, and characterizing biodiversity. Non-invasively collected samples
60 are easier to obtain than fresh organ tissues, but may contain PCR inhibitors, have lower DNA
61 yields, or are degraded from environmental exposure (Kohn, Knauer, Stoffella, Schröder, &
62 Pääbo, 1995; Rådström, Knutsson, Wolffs, Lövenklev, & Löfström, 2004; Waits & Paetkau,
63 2005; Chaturvedi et al., 2008). Archived historical wildlife samples, often preserved in formalin,
64 also offer a unique opportunity to obtain genetic information (Seimon et al., 2015). However,
65 challenges for molecular studies include formalin-related fragmentation and DNA cross-linking
66 (Do & Dobrovic, 2015; Einaga et al., 2017).
67
68 DNA barcoding is a common molecular technique for species identification (Hebert,
69 Ratnasingham, & de Waard, 2003; Valentini, Pompanon, & Taberlet, 2009). The Oxford
70 Nanopore Technologies (ONT) MinION sequencer is currently the only available portable
71 sequencer. Although nanopore sequencing is known to have higher raw sequence error rates in
72 comparison to standard short read sequencing platforms such as Illumina or BGI-Seq,
73 particularly at homopolymeric regions (Ip et al., 2015; Jain et al., 2017), significant
74 improvements in the accuracy of MinION sequencing chemistry has led to its recent rise in
75 popularity for field applications (reviewed in Krehenwinkel, Pomerantz, & Prost, 2019). This
76 sequencer is especially useful in situations where there is a lack of access to sequencing facilities
77 or when sample export is difficult. The MinION also has a lower investment cost and shorter
78 turnaround times than traditional sequencing platforms (e.g., Sanger, Illumina).
79

80 MinION DNA barcoding studies have primarily used laboratory-based QIAGEN® kits for
81 reliable and pure DNA extraction products (e.g., Pomerantz et al., 2018; Krehenwinkel,
82 Pomerantz, Henderson, et al., 2019; Maestri et al., 2019). To expand the potential for portable
83 sequencing applications, field-friendly DNA extraction methods can be used to reduce lab
84 equipment requirements. While field-friendly DNA extraction methods are often less effective at
85 producing DNA of high concentration and purity levels, MinION DNA barcoding has been
86 successfully performed using QuickExtract™ solution (Lucigen), which only requires a heat
87 source (Srivathsan et al., 2019). The Chelex® 100 resin (Bio-Rad Inc.) extraction method
88 similarly only requires a heat source, but is less expensive and has not been tested for MinION
89 sequencing so far. Both methods have short protocols, but do not remove cellular debris or PCR
90 inhibitors, which can affect downstream applications (Walsh, Metzger, & Higuchi, 1991; Singh,
91 Kumari, & Iyengar, 2018). The Biomeme M1 Sample Prep™ Kit (Biomeme Inc.) is another
92 DNA extraction kit developed for field use. While more expensive than either QuickExtract or
93 Chelex methods, the Biomeme kit includes all necessary components and both protein and salt
94 wash steps to remove impurities. Studies have shown that Biomeme-extracted samples have
95 higher levels of inhibitors compared to Qiagen extractions, and thus requires additional dilution
96 steps (Sepulveda, Hutchins, Massengill, & Dunker, 2018; Thomas et al., 2019).
97
98 To date, MinION DNA barcoding pipelines have used either *de novo* assembly (Pomerantz et al.,
99 2018; Krehenwinkel, Pomerantz, Henderson, et al., 2019), clustering-based (Maestri et al.,
100 2019), or alignment (Srivathsan et al., 2018, 2019) methods to generate consensus sequences for
101 species identification. Assembly approaches generally work more consistently for longer
102 barcodes (~1kb), as the underlying software were originally designed for assembling long reads

103 for genome assemblies rather than amplicons. Both published clustering or alignment pipelines
104 use subsets of the data (100-200 reads) to generate scaffolds for read error correction. While
105 these approaches may work for high quality sequence data, the data subsets could include more
106 sequence error bias in lower quality datasets. Thus, we developed a clustering-based pipeline,
107 SAIGA (https://github.com/marisalim/Saiga), with software specifically designed for error prone
108 MinION reads that processes data regardless of barcode length, and maximizes the use of
109 demultiplexed reads for downstream species identification analysis.
110
111 In this study, we systematically evaluate the accuracy of the MinION for DNA barcoding across
112 a range of wildlife sample types, including two field-friendly DNA extraction approaches. We
113 sequenced a short fragment of the commonly used mitochondrial cytochrome b (Cytb) gene from
114 scat, hair, feather, fresh frozen liver and formalin-fixed paraffin embedded (FFPE) liver. For
115 each sample type, we compared the accuracy of Cytb consensus sequences for three different
116 DNA extraction methods: QIAGEN silica membrane-based kits, Chelex 100 resin, and the
117 Biomeme M1 Sample Prep Kit. All analyses were conducted with SAIGA. We demonstrate that
118 MinION sequencing can be used with field-friendly extraction methods to accurately identify
119 wildlife species from a variety of sample types.
120
121 **Materials and Methods**
122 **Sample collection**
123 For this study, scat, hair, feather, fresh frozen liver and FFPE liver samples were collected
124 opportunistically during necropsy examinations from a snow leopard (*Panthera uncia*) and a
125 cinnamon teal (*Anas cyanoptera*) from a zoological collection. The FFPE liver samples were part

126 of a suite of tissues that were collected, stored in 10% neutral buffered formalin, and
127 subsequently processed and paraffin-embedded for histologic examination and routine tissue
128 archiving. Fresh liver, scat, hair and feather samples were frozen (-80°C) immediately after
129 collection.
130
131 **DNA extraction**
132 DNA was extracted from each sample type using three different approaches: 1) Qiagen
133 (QIAamp® DNA minikit or QIAamp® DNA Stool Mini Kit, Qiagen Inc., Germantown, MD,
134 USA); 2) Chelex 100 Resin (Bio-Rad, Hercules, CA, USA); and 3) Biomeme M1 Sample Prep
135 Kit for DNA (Biomeme, Philadelphia, PA, USA). DNA quantification is inaccurate for Chelex
136 extracts due to the presence of cellular components, thus Chelex extracts were not quantified. All
137 Qiagen and Biomeme extracts were quantified using the Qubit™ dsDNA High Sensitivity Kit on
138 the Qubit™ 4 Fluorometer (Thermo Fisher Scientific, Waltham, MA, USA). The Qiagen,
139 Chelex, and Biomeme extraction protocols are summarized for each tissue type in Appendix I.
140 All Qiagen, Biomeme DNA extracts with >10ng/µL, and all Chelex extracts were run on a 1.0%
141 gel to assess DNA fragmentation by sample type.
142
143 **PCR & library preparation**
144 *DNA Barcoding PCR - Round 1*
145 Approximately 460 bp of the mitochondrial Cytb gene was amplified using primers mcb398 and
146 mcb869 (Verma & Singh, 2003), with universal tailed sequences on each primer that are
147 compatible with the ONT PCR Barcoding Expansion kit EXP-PBC001 (ONT, Oxford, UK)

148 (Table S1). These primers were designed from an alignment of 67 animal species, and validated
149 for mammals, reptiles and birds (Verma & Singh, 2003).
150
151 PCR was carried out with 6.25 µL DreamTaq HotStart PCR Master Mix (Thermo Fisher,
152 Waltham, MA, USA), 1.25 µL DNA template, and 2 µL of each primer (10 µM stock) in a final
153 volume of 12.5 µL. Cycling conditions were: 95°C for 3 minutes; 35 cycles of 95°C for 30
154 seconds, 55°C for 30 seconds and 72°C for 30 seconds; and a final extension of 72°C for 5
155 minutes. All Chelex extractions were diluted for the DNA Barcoding PCR as described in
156 Appendix I. PCR products were purified using 1.8X Agencourt AMPure XP beads (Beckman
157 Coulter, Indianapolis, IN, USA), tested for purity using the NanoDrop™ One spectrophotometer
158 (Thermo Fisher Scientific, Waltham, MA, USA), and quantified fluorometrically using the Qubit
159 dsDNA High sensitivity kit.
160
161 *Indexing PCR - Round 2*
162 To attach dual ONT PCR index sequences to the Cytb amplicons, a second round of PCR was
163 carried out with the ONT PCR Barcoding Expansion kit for each sample with 25 µL KAPA
164 Biosystems HiFi HotStart ReadyMix (2X) (Thermo Fisher Scientific, Waltham, USA),
165 containing 25 ng of first-round PCR amplicon and 1 µL ONT PCR Barcode in a final volume of
166 50 µL. Cycling conditions were: 95°C for 3 minutes; 11 cycles of 95°C for 15 seconds, 62°C for
167 15 seconds and 72°C for 15 seconds; and a final extension of 72°C for 1 minute. Hereafter, we
168 refer to ONT PCR barcodes as 'indexes' to reduce confusion with the Cytb barcode. Indexed
169 PCR products from round 2 were purified and tested for purity and quantity like round 1
170 products.

171

172 *Library preparation*

173 Samples were grouped into four libraries by sample type (FFPE, scat, hair/feather, frozen liver).
174 For each library, purified indexed amplicons were pooled in equal ratios to produce 1.0-1.2 µg in
175 a total of 45 µL nuclease-free water. Pooled libraries were next prepared using the ONT Ligation
176 Sequencing kit SQK-LSK109 (ONT, Oxford, UK) with modifications to the manufacturer's
177 instructions: 25 µL of the pooled library was mixed with 3.5 µL NEBNext Ultra II End-Prep
178 Reaction buffer and 1.5 µL Ultra II End-prep Enzyme mix (New England Biolabs, Ipswich, MA,
179 USA), incubated for 10 minutes at room temperature, then 10 minutes at 65°C. For adapter
180 ligation, 15 µL of the end-prepped library (not bead-purified) was mixed with 25 µL Blunt/TA
181 Ligase and 10 µL Adapter Mix (AMX), incubated at room temperature for 20 minutes and eluted
182 in a final volume of 12 µL of Elution Buffer.

183

184 **Sequencing**

185 The four libraries were split between two FLO-MIN106D R9.4.1 chemistry flow cells (ONT,
186 Oxford, UK) - to minimize bleed-through between experiments - FAL19910: 1) FFPE, 2) scat;
187 FAL19272: 1) hair/feather, 2) frozen liver. Flow cells were washed with Wash Solution A
188 followed by the addition of Storage buffer S according to the manufacturer's protocols. All
189 libraries were sequenced for approximately 1 hour to obtain at least 100,000 raw reads per
190 sample.

191

192 For comparison to MinION sequences, Sanger sequencing in the forward and reverse directions
193 was performed on all purified indexed amplicons (Eton Bioscience Inc. Newark, NJ, USA).

194 Sanger consensus sequences were generated using Geneious Prime v2019.0.4 software
195 (Biomatters LDT, Auckland, NZ).
196
197 **Bioinformatics**
198 The SAIGA bioinformatics pipeline is available on GitHub (https://github.com/marisalim/Saiga)
199 and steps are outlined in Fig. 1. MinKNOW (ONT) was used for sequencing and the raw
200 sequence data were basecalled using Guppy v3.5.1 (ONT) with basecalling model
201 "dna_r9.4.1_450bps_fast.cfg".
202
203 *Demultiplexing and filtering*
204 Assigning sequencing reads to the correct sample is a critical step to avoid mixing sample
205 sequences within or between sequencing runs. Thus, we compared results from two
206 demultiplexing programs: 1) qcat v1.1.0 (ONT, https://github.com/nanoporetech/qcat) and 2)
207 MiniBar v0.21 (Krehenwinkel, Pomerantz, Henderson, et al., 2019). The qcat software was built
208 specifically for demultiplexing reads indexed with ONT's barcode kits, while MiniBar is a
209 general demultiplexing software that allows any set of user-specified index and primer
210 sequences. We used stringent demultiplexing filters based on software recommendations,
211 sensitivity analyses, and to minimize incorrect read assignments. Qcat uses the epi2me
212 demultiplexing algorithm and we trimmed adapter and index sequences with the trim option.
213 Using the min-score option, demultiplexed reads with alignment scores <99 were removed prior
214 to downstream analysis, where a score of 100 means every nucleotide of the index is correct.
215 Lower min-score thresholds (i.e., 60-90) reduced downstream consensus sequence quality. In
216 MiniBar, up to 2 nucleotide differences between reads were allowed for the index sequences and

217 11 nucleotide differences between primer sequences per software recommendations; MiniBar
218 primarily uses the index sequence information to demultiplex and trim dual index and primer
219 sequence.
220
221 After demultiplexing, reads were removed if they had mean Phred quality scores <7 and were
222 longer or shorter than the target amplicon length (~421 bp excluding primers) with a 100 bp
223 buffer (321-521 bp) in NanoFilt v2.5.0 (De Coster, D'Hert, Schultz, Cruts, & Van Broeckhoven,
224 2018). Following each of the above steps, we calculated and visualized read quality statistics for
225 raw, demultiplexed, and filtered reads with NanoPlot v1.21.0 (De Coster et al., 2018). To
226 standardize dataset size across the four sequencing experiments and to investigate the effect of
227 read depth, we generated 100, 500, and 5,000 random read subsets for each sample from the
228 filtered demultiplexed read files. Hereafter, we refer to these subsets as 100R, 500R, and 5KR,
229 respectively.
230
231 *Read clustering and consensus sequence generation*
232 To generate the consensus sequence for each sample, all reads were first clustered using
233 isONclust v0.0.4 (Sahlin & Medvedev, 2018). We chose isONclust over clustering tools
234 previously used in nanopore-based DNA barcoding pipelines, such as VSEARCH (implemented
235 in ONTrack, Maestri et al., 2019), as it was specifically designed to work with error-prone long-
236 read data and thus should be less affected by read errors and more efficient in cluster formation.
237 Next, SAIGA outputs the number of reads per cluster, only retaining clusters with >10% of the
238 total reads (user-defined). We implemented this step to minimize the inclusion of reads with high
239 sequence error and possible contaminant reads in downstream analysis. Intermediate consensus

240 sequences are then generated using SPOA v3.0.1 (https://github.com/rvaser/spoa), which is
241 based on a partial order alignment (POA) algorithm (Lee, 2003). SPOA also conducts error
242 corrections, resulting in more accurate consensus sequences. The SPOA consensus sequences are
243 then clustered using cd-hit-est v4.8.1 with a stringent similarity cutoff (0.9; user-defined) (Li &
244 Godzik, 2006; Fu, Niu, Zhu, Wu, & Li, 2012). Since isONclust separates reads in different strand
245 orientations, this second round of clustering groups reverse-complement SPOA consensus
246 sequences, ensuring that more filtered reads are used for generating the final consensus
247 sequence. The reads contributing to all SPOA consensus sequences that group with the majority
248 isONclust cluster's SPOA consensus sequence are combined into a single file for mapping.
249 SAIGA then maps these reads to the SPOA consensus sequence of the majority isONclust cluster
250 for consensus polishing with ONT's Medaka software v0.10.0
251 (https://github.com/nanoporetech/medaka).
252
253 **Consensus accuracy and analysis**
254 The MinION consensus sequences were compared to Sanger sequences from the same sample
255 using a nucleotide Blast search v2.8.1+ (Altschul, Gish, Miller, Myers, & Lipman, 1990). To
256 assess and compare species identification results across tissue types, extraction methods,
257 demultiplexing programs, and data subsets, the following were evaluated: 1) the percent of
258 matching nucleotides between consensus and Sanger sequences, 2) the number of matching
259 nucleotides between consensus and Sanger sequences, and 3) the proportion of filtered reads in
260 the cluster used to generate final consensus sequence. Accurate species identification was
261 defined as those with >99% sequence similarity to the Sanger sequence and ~421 bp of matching
262 nucleotides. The proportion of demultiplexed reads contributing to the final consensus indicates

263 how much data was used for species identification. For samples with consensus sequences
264 generated from fewer than ~75% of reads, we investigated the non-majority isONclust clusters
265 for potential sequence error or contaminant reads. Finally, all MinION consensus and Sanger
266 sequences across tissue types, extraction methods, demultiplexing software, and data subsets
267 were aligned with Mafft v1.3.7 in Geneious Prime v2019.0.4 to identify common regions with
268 sequence errors.
269
270 **Results**
271 **DNA Barcoding and Indexing PCR performance**
272 DNA concentrations were higher for Qiagen (0.8 to 59 ng/µL, n=8) compared to Biomeme (0.07
273 to 13.9 ng/µL, n=8) extractions (Table S2); Chelex samples were not quantified (n=8). Gel
274 electrophoresis of Qiagen-extracted tissues show frozen liver and scat samples had high
275 molecular weight genomic DNA, while FFPE samples were fragmented; hair and feather extracts
276 were too faint to detect reliably. (Fig. S1). We were unable to detect high molecular weight
277 nucleic acid in the Biomeme and Chelex-extracted samples (Fig. S2). Despite variation in
278 starting DNA concentration and the presence of low molecular weight fragments in some
279 samples, we successfully barcoded and indexed 22 of 24 samples. The two samples that failed to
280 amplify at the Barcoding PCR (Round 1) step were the snow leopard FFPE samples extracted by
281 the Chelex and Biomeme protocols. The DNA concentration of DNA Barcoding PCR (Round 1)
282 products after bead clean-up was <13.9 ng/µL with an average of 3.49 ng/µL. At these low DNA
283 concentrations, NanoDrop purity of Barcoding Round 1 amplicons is highly variable and not
284 reliable.
285

286 Two samples had less than 25 ng for Indexing PCR (Round 2). After bead clean-up, the
287 concentration of the snow leopard liver/Chelex DNA Barcoding PCR (Round 1) product was
288 much lower than expected (4.4 ng), despite having a bright agarose gel band. Nevertheless, this
289 was sufficient for amplification in the Indexing PCR step. Cytb was also difficult to amplify
290 from the snow leopard scat/Chelex, so amplicons from two DNA Barcoding (Round 1) PCR
291 reactions were pooled for a total of 16 ng to proceed with Indexing PCR (Round 2). After the
292 Indexing PCR (Round 2) bead clean-up, DNA concentrations were >19 ng/µL with an average of
293 80.92 ng/µL for all but the snow leopard liver/Chelex sample, which had 6.58 ng/µL. Average
294 A260/280 ratios (1.82) and A260/230 ratios (1.96) indicated relatively pure samples for library
295 preparation.
296
297 **MinION and Sanger sequencing performance**
298 Sequencing efficiency, also called pore occupancy, ranged from 72-80% and was evenly spread
299 across flow cells for all MinION sequencing runs (Fig. S3). We sequenced an average of
300 ~752,856 raw reads per run, with an average read length of ~597 bp and read quality Phred score
301 of 10.5 (Table S3, Fig. S4).
302
303 We obtained clean Sanger sequences for 21 of 22 samples, all of which were 421 bp after primer
304 trimming (Table S4). For all 21 samples, the Sanger sequences for each species were identical,
305 regardless of tissue type or extraction method. We were unable to get a clean Sanger sequence
306 for the snow leopard scat/Chelex sample. Therefore, we compared the MinION scat/Chelex
307 consensus to the Sanger sequences from the other snow leopard samples for species identity.
308

309 **Sequence read retention after demultiplexing and filtering**

310 The average read quality and read lengths were similar across all samples demultiplexed with
311 MiniBar or qcat (Table S3-S4). For all sequencing runs, both MiniBar and qcat correctly
312 assigned demultiplexed reads only to the ONT indexes used in the Indexing PCR for each run
313 (Fig. 2). Due to the stringent demultiplexing thresholds, the majority of read data loss occurred
314 during the demultiplexing step (84.07% reads lost on average; Table S3). After read quality and
315 length filtering, we retained nearly all demultiplexed reads (95.6% reads retained on average;
316 Fig. S5, Table S3). On average, samples had more than 20,000 demultiplexed and filtered reads
317 for downstream analyses (Table S4). In general, MiniBar-demultiplexed datasets retained more
318 reads than qcat-demultiplexed datasets after filtering (Fig. S5). The only sample that retained
319 fewer than 90% of reads after filtering was the cinnamon teal scat/Biomeme sample
320 demultiplexed with MiniBar (68.90% reads retained).

321

322 **Read clustering proportions and cluster species identity**

323 For nearly all data subsets, there were only two isONclust clusters for each sample comprising
324 forward and reverse-complement oriented reads. In these cases, 100% of filtered reads formed a
325 single cluster after cd-hit clustering (to merge potential reverse-complements) and all reads were
326 used to produce the consensus sequence for final species identification (Fig. 3).

327

328 In the remaining 18 data subsets, there were two categories: 1) samples where fewer than 60% of
329 reads were used for final consensus generation due to sequence error and 2) samples with
330 clusters containing contaminant reads (Table S5). In 5KR subsets for three cinnamon teal
331 (FFPE/Chelex, liver/Biomeme, scat/Biomeme) and two snow leopard (hair/Qiagen, liver/Qiagen)

332 samples, the second largest isONclust cluster contained reads that best match the same species as
333 the majority cluster. While SPOA consensus sequences for these two clusters remained separate
334 after cd-hit-est clustering, likely due to sequencing error (Table S5), species identification was
335 successful for these five 5KR subset samples using only ~50% of the reads to build the
336 consensus. In comparison, 100% of the reads clustered for the 100R and 500R subsets for these
337 samples, suggesting that the 5KR subsample contained slightly more variation in read quality
338 than the smaller subsets.
339
340 We detected low to medium levels of cinnamon teal reads in three snow leopard samples:
341 hair/Qiagen, scat/Chelex, and liver/Chelex, where the full set of demultiplexed reads contained
342 3.9%, 22.0%, and 14.4% teal reads, respectively. There were no teal contaminant reads, and
343 hence no teal read clusters, in the snow leopard hair/Qiagen sample for all subsets. In contrast,
344 the proportions of reads used to generate final consensus for all subsets of the snow leopard
345 scat/Chelex and liver/Chelex samples were reduced to 75-85% of reads (Table S5). Recovery of
346 DNA Barcoding PCR (Round 1) products was low for these two samples. However, our
347 pipeline's filtering and clustering procedures were able to correctly identify these samples as
348 snow leopard because reads with high sequence errors and contaminant reads were not included
349 in downstream analysis. There were no cinnamon teal reads in the rest of the snow leopard
350 samples, and no snow leopard reads in any cinnamon teal samples.
351
352 **Consensus sequence generation**
353 The average proportion of reads used and consensus sequence lengths were comparable between
354 sample types, extraction methods, subsets and demultiplexers (Table 1, Table S6). In general,

355 SAIGA retained similar proportions of reads to generate consensus sequences across samples
356 extracted by the Biomeme and Chelex methods as compared to the gold standard Qiagen-
357 extracted samples (Fig. 3, Table 1, Table S6). In two cases, greater proportions of reads were
358 used for the snow leopard liver and hair samples extracted with the Biomeme and Chelex
359 protocols compared to the Qiagen-extract of the same tissue type. For samples where the
360 consensus sequence length differed by demultiplexer, MiniBar subsets produced slightly longer
361 sequences than qcat subsets (Fig. S6).
362
363 **Validation of sample species identity**
364 The average sequence similarity between MinION consensus sequences and their corresponding
365 Sanger sequence was highly accurate (>99.29% match) and remarkably consistent across sample
366 type, extraction method, subset, and demultiplexer (Fig. 4, Table 1). There was slightly more
367 variation in sequence similarity across 5KR subsets, with the overall lowest percent sequence
368 match (99.29%) obtained in these subsets for the cinnamon teal scat/Biomeme sample. This
369 sample also had lower read cluster proportions (Fig. 3) and the greatest loss in data after filtering
370 (Fig. S5).
371
372 The MinION consensus sequences from both MiniBar- and qcat-demultiplexed subsets extended
373 into the Cytb primer region. We trimmed away the primers from both Sanger and MinION
374 consensus sequences for Mafft alignment of all samples. The cinnamon teal alignment had
375 99.8% pairwise identity and 97.2% identical sites (n=84 sequences), while the snow leopard
376 alignment had 99.9% pairwise identity and 98.6% identical sites (n=69 sequences). The MinION

377 consensus and Sanger sequences for each animal mainly differed at the ends of the sequences
378 and at homopolymeric regions of varying lengths within the sequence (Table S7, Fig. 5).
379
380 **Discussion**
381 We demonstrate that a MinION-based DNA barcoding workflow can generate accurate
382 consensus sequences from scat, hair, feather, and FFPE liver tissue samples, which are often
383 considered challenging for molecular studies. The ability to use field-friendly DNA extraction
384 protocols with these sample types will help to overcome logistical challenges, such as the need
385 for cumbersome or expensive equipment, for molecular field research. The accuracy of our
386 species identifications is on par with previous MinION DNA barcoding studies and pipelines
387 (Pomerantz et al., 2018; Srivathsan et al., 2018, 2019; Krehenwinkel, Pomerantz, Henderson, et
388 al., 2019; Maestri et al., 2019). For all tissue types, extraction methods, and subsets tested with
389 our pipeline, we obtained high quality reads and a consensus sequence that matched >99.29%
390 and at least 419/421 bp to the Sanger sequence for each sample. Although Oxford Nanopore's
391 goal is the "analysis of any living thing, by anyone, anywhere," major barriers to its use are ease
392 of sample processing, complicated data analysis, and cost. The results of our study help to reduce
393 these barriers.
394
395 *Field-friendly protocols for wildlife samples expands conservation applications with the MinION*
396 We show that the Chelex and Biomeme extraction methods can be used to generate highly
397 accurate MinION consensus sequences, similar to Qiagen extraction methods, even with low
398 starting DNA concentrations. Our PCR amplicon purification and library prep protocols resulted
399 in libraries of sufficient purity; cellular debris or contaminants present in the Chelex and

400 Biomeme extracts did not affect sequencing of the Cytb amplicons. Although the field-friendly
401 DNA extracts had low DNA concentrations overall, amplification was successful for all samples,
402 including scat (known for containing PCR inhibitors), hair and feather (low DNA quantities),
403 and FFPE tissue, from which DNA is generally difficult to amplify.
404
405 Formalin can cause DNA fragmentation, cross-linking, subsequent sequence artifacts and altered
406 base pairs (Do & Dobrovic, 2015; Einaga et al., 2017). As artifacts are randomly distributed,
407 they should not affect the final Sanger sequence if sufficient starting template is used
408 (Srinivasan, Sedmak, & Jewell, 2002; Quach, Goodman, & Shibata, 2004). Indeed, we
409 accurately sequenced Qiagen-extracted DNA from FFPE samples, and further show that
410 amplifiable DNA was successfully isolated from FFPE tissue using Chelex and Biomeme
411 extraction methods.
412
413 *SAIGA: A DNA barcoding bioinformatics pipeline for new MinION users*
414 We developed the SAIGA bioinformatics pipeline with a read clustering and consensus calling
415 approach using software that were specifically designed for long-read and error-prone sequence
416 data (isONclust, SPOA, Medaka). SAIGA performed successfully and consistently with as few
417 as 100 reads per sample, allowing researchers to reduce sequencing time and cost per sample
418 (e.g., multiplexing more samples). Like other studies investigating read coverage requirements,
419 species identification accuracy still met our requirements but dropped slightly for the larger
420 subset (5KR) (Pomerantz et al., 2018; Krehenwinkel, Pomerantz, Henderson, et al., 2019).
421 Further, SAIGA options allow users to explore parameters and provide informative data quality

422 checks and statistics throughout the pipeline. All software components are freely available and
423 the pipeline structure allows for integration of new software in the future.
424
425 Our results show that both qcat and MiniBar correctly demultiplex reads between samples in a
426 sequence run and across multiple runs on a flow cell. Due to the very stringent demultiplexing
427 parameters, the majority of raw data loss occurred during read assignment. More relaxed settings
428 reduce raw read loss, but increase the chance of including incorrectly assigned reads or reads
429 with higher sequencing error. Srivathsan et al. (2019) and Maestri et al. (2019) noted similar
430 magnitudes of read loss with ~76% and ~53.6% of reads lost after demultiplexing, respectively;
431 other MinION DNA barcoding publications have not reported this statistic. Despite the read loss,
432 MiniBar- and qcat-demultiplexed reads performed well based on all our metrics for accurate
433 species identification. Both demultiplexers tend to under-trim reads, which is preferred since
434 potentially useful regions of the amplicon for distinguishing species are lost from over-trimmed
435 reads. Although the consensus accuracy of qcat results was slightly higher than MiniBar results,
436 we prefer Minibar for its flexibility to analyze non-ONT index sequences. Customized indexes
437 are less expensive than ONT indexes and can be lyophilized for field use.
438
439 Measuring the proportion of clustered filtered reads used for consensus sequence generation
440 provides a benchmark for detecting sequencing error and potential contamination. For example,
441 SAIGA created separate SPOA consensus sequence clusters for some samples even though these
442 clusters produce the same species identification result. Lowering the sequence similarity
443 threshold in cd-hit could force the sequences to form a single cluster. However, for the purpose
444 of validating SAIGA, we used very stringent sequence similarity thresholds to reduce species

445 identification bias from sequence error. Using this measure, we also show that SAIGA can
446 handle low to medium amounts of laboratory contamination (~4-20% reads of total subsample)
447 from relatively distinct species in samples without affecting final species identification since
448 contaminant reads were successfully filtered out during the clustering process. Since contaminant
449 teal reads had the correct indexes used for the three snow leopard samples, contamination likely
450 occurred during library preparation rather than from mis-assignment of reads during
451 demultiplexing. These snow leopard samples were either difficult to amplify during the
452 Barcoding PCR (scat/Chelex) or had low recovery of indexed PCR product used in the
453 sequencing run (hair/Biomeme and liver/Chelex). The contamination risk for these samples was
454 likely exacerbated by the two-step PCR protocol and low starting DNA concentration and/or
455 purity. Further development is needed to adapt this workflow and pipeline for mixed species
456 samples, for which it may be more difficult to differentiate between true sample species and
457 laboratory contaminants.
458
459 *Cost-effective strategies for field implementation*
460 Each field-friendly method has its advantages and disadvantages. The Chelex method is cheap
461 and the resin can be transported at room temperature, but requires heating equipment and the
462 Chelex solution must be kept cool (4°C) once prepared. The Biomeme kit is room temperature
463 stable and self-contained. However, it is more expensive than both the Chelex resin and Qiagen
464 kits ($15/sample versus $0.17 and $3, respectively) and yielded lower DNA concentrations
465 compared to the Qiagen kit.
466

467 We show that qcat and MiniBar can correctly assign reads to samples within and between runs,
468 which reduces costs by allowing multiple sequence runs per flow cell. Future experiments can
469 also scale up by sequencing more samples per flow cell because relatively few reads per sample
470 are required for a consistent, accurate consensus (e.g. Srivathsan et al., 2019). For the Cytb
471 barcode amplified in this study, reads were sequenced at a rate of ~100,000 reads per ~10
472 minutes. Sufficient sequence data for species barcoding can therefore be obtained rapidly
473 depending on the barcoding gene length and number of samples. We also reduced the volumes of
474 the ONT PCR index per sample by 50% to lower costs and maximize the ONT kit.
475

476 **Conclusions**

477 Portable sequencing technology and field-friendly protocols have incredible potential to
478 overcome institutional and geographical obstacles that impede genetic analyses in wildlife
479 conservation and animal health. The methods described here provide an easy-to-follow workflow
480 using field-friendly DNA extraction methods that can be used for preserved and non-invasively
481 collected wildlife sample types to produce high-quality consensus sequences for species
482 identification. Future studies are necessary to develop additional field-friendly protocols to
483 further reduce the need for cold chain requirements, scale up sample processing, and tackle
484 samples of mixed species, which will help to increase the opportunities for implementation.
485

486 **Acknowledgements**

487 Funding was provided by the G. Unger Vetlesen Foundation. We thank Nina Vasiljevic and Rob
488 Ogden for sharing their library preparation protocol and valuable discussions for our informatics

489 pipeline, Batya Nightingale for lab assistance, and two anonymous reviewers for helpful
490 comments.
491

492 **Author Contributions**

493 AS and MCWL contributed equally to the project. AS, MCWL, DM, SP, and TS designed the
494 study and interpreted the data. SP and MCWL developed SAIGA. AS conducted the lab work.
495 MCWL performed the bioinformatics analysis. All authors contributed to writing the draft and
496 gave final approval for publication.
497

498 **Data Availability**

499 A representative Sanger sequence for both species is available on GenBank (MN823069-70), and
500 MinION fastq files (basecalled, demultiplexed, and filtered) are available on NCBI Short Read
501 Archive (BioProject: PRJNA594927, accessions: SRR10678113-SRR10678156). Raw MinION
502 sequence data is available on the EBI European Nucleotide Archive (ERP119594).
503

504 **References**

505 Altschul, S. F., Gish, W., Miller, W., Myers, E. W., & Lipman, D. J. (1990). Basic local
506 alignment search tool. *Journal of Molecular Biology*, *215*(3), 403–410.
507 doi:10.1016/S0022-2836(05)80360-2
508 Chaturvedi, U., Tiwari, A. K., Ratta, B., Ravindra, P. V., Rajawat, Y. S., Palia, S. K., & Rai, A.
509 (2008). Detection of canine adenoviral infections in urine and faeces by the polymerase
510 chain reaction. *Journal of Virological Methods*, *149*(2), 260–263.
511 doi:10.1016/j.jviromet.2008.01.024

512 Costa, F. O., & Carvalho, G. R. (2007). The Barcode of Life Initiative: synopsis and prospective
513 societal impacts of DNA barcoding of Fish. *Genomics, Society and Policy*, *3*(2), 29.
514 doi:10.1186/1746-5354-3-2-29
515 De Barba, M., Miquel, C., Boyer, F., Mercier, C., Rioux, D., Coissac, E., & Taberlet, P. (2014).
516 DNA metabarcoding multiplexing and validation of data accuracy for diet assessment:
517 application to omnivorous diet. *Molecular Ecology Resources*, *14*(2), 306–323.
518 doi:10.1111/1755-0998.12188
519 De Coster, W., D'Hert, S., Schultz, D. T., Cruts, M., & Van Broeckhoven, C. (2018). NanoPack:
520 visualizing and processing long-read sequencing data. *Bioinformatics*, *34*(15), 2666–
521 2669. doi:10.1093/bioinformatics/bty149
522 Do, H., & Dobrovic, A. (2015). Sequence Artifacts in DNA from Formalin-Fixed Tissues:
523 Causes and Strategies for Minimization. *Clinical Chemistry*, *61*(1), 64–71.
524 doi:10.1373/clinchem.2014.223040
525 Einaga, N., Yoshida, A., Noda, H., Suemitsu, M., Nakayama, Y., Sakurada, A., … Esumi, M.
526 (2017). Assessment of the quality of DNA from various formalin-fixed paraffin-
527 embedded (FFPE) tissues and the use of this DNA for next-generation sequencing (NGS)
528 with no artifactual mutation. *PLoS ONE*, *12*(5). doi:10.1371/journal.pone.0176280
529 Ficetola, G. F., Miaud, C., Pompanon, F., & Taberlet, P. (2008). Species detection using
530 environmental DNA from water samples. *Biology Letters*, *4*(4), 423–425.
531 doi:10.1098/rsbl.2008.0118
532 Fu, L., Niu, B., Zhu, Z., Wu, S., & Li, W. (2012). CD-HIT: accelerated for clustering the next-
533 generation sequencing data. *Bioinformatics (Oxford, England)*, *28*(23), 3150–3152.
534 doi:10.1093/bioinformatics/bts565

535 Galimberti, A., Casiraghi, M., Bruni, I., Guzzetti, L., Cortis, P., Berterame, N. M., & Labra, M.
536 (2019). From DNA barcoding to personalized nutrition: the evolution of food traceability.
537 *Current Opinion in Food Science*, *28*, 41–48. doi:10.1016/j.cofs.2019.07.008
538 Gardy, J. L., & Loman, N. J. (2018). Towards a genomics-informed, real-time, global pathogen
539 surveillance system. *Nature Reviews Genetics*, *19*(1), 9–20. doi:10.1038/nrg.2017.88
540 Hebert, P. D. N., Ratnasingham, S., & de Waard, J. R. (2003). Barcoding animal life:
541 cytochrome c oxidase subunit 1 divergences among closely related species. *Proceedings*
542 *of the Royal Society of London. Series B: Biological Sciences*, *270*(suppl_1), S96–S99.
543 doi:10.1098/rsbl.2003.0025
544 Hobbs, C. A. D., Potts, R. W. A., Walsh, M. B., Usher, J., & Griffiths, A. M. (2019). Using DNA
545 Barcoding to Investigate Patterns of Species Utilisation in UK Shark Products Reveals
546 Threatened Species on Sale. *Scientific Reports*, *9*(1), 1–10. doi:10.1038/s41598-018-
547 38270-3
548 Ip, C. L. C., Loose, M., Tyson, J. R., de Cesare, M., Brown, B. L., Jain, M., … Olsen, H. E.
549 (2015). MinION Analysis and Reference Consortium: Phase 1 data release and analysis.
550 *F1000Research*, *4*. doi:10.12688/f1000research.7201.1
551 Jain, M., Tyson, J. R., Loose, M., Ip, C. L. C., Eccles, D. A., O'Grady, J., … Olsen, H. E. (2017).
552 MinION Analysis and Reference Consortium: Phase 2 data release and analysis of R9.0
553 chemistry. *F1000Research*, *6*. doi:10.12688/f1000research.11354.1
554 Kohn, M., Knauer, F., Stoffella, A., Schröder, W., & Pääbo, S. (1995). Conservation genetics of
555 the European brown bear - a study using excremental PCR of nuclear and mitochondrial
556 sequences. *Molecular Ecology*, *4*(1), 95–104. doi:10.1111/j.1365-294X.1995.tb00196.x

Krehenwinkel, H., Pomerantz, A., Henderson, J. B., Kennedy, S. R., Lim, J. Y., Swamy, V., … Prost, S. (2019). Nanopore sequencing of long ribosomal DNA amplicons enables portable and simple biodiversity assessments with high phylogenetic resolution across broad taxonomic scale. *GigaScience*, *8*(5), giz006. doi:10.1093/gigascience/giz006

Krehenwinkel, Pomerantz, & Prost. (2019). Genetic Biomonitoring and Biodiversity Assessment Using Portable Sequencing Technologies: Current Uses and Future Directions. *Genes*, *10*(11), 858. doi:10.3390/genes10110858

Lee, C. (2003). Generating consensus sequences from partial order multiple sequence alignment graphs. *Bioinformatics*, *19*(8), 999–1008. doi:10.1093/bioinformatics/btg109

Li, W., & Godzik, A. (2006). Cd-hit: a fast program for clustering and comparing large sets of protein or nucleotide sequences. *Bioinformatics (Oxford, England)*, *22*(13), 1658–1659. doi:10.1093/bioinformatics/btl158

Maestri, S., Cosentino, E., Paterno, M., Freitag, H., Garces, J. M., Marcolungo, L., … Delledonne, M. (2019). A Rapid and Accurate MinION-Based Workflow for Tracking Species Biodiversity in the Field. *Genes*, *10*(6), 468. doi:10.3390/genes10060468

Marshall, H. D., & Ritland, K. (2002). Genetic diversity and differentiation of Kermode bear populations. *Molecular Ecology*, *11*(4), 685–697. doi:10.1046/j.1365-294x.2002.01479.x

Pardo, M. Á., Jiménez, E., Viðarsson, J. R., Ólafsson, K., Ólafsdóttir, G., Daníelsdóttir, A. K., & Pérez-Villareal, B. (2018). DNA barcoding revealing mislabeling of seafood in European mass caterings. *Food Control*, *92*, 7–16. doi:10.1016/j.foodcont.2018.04.044

Pomerantz, A., Peñafiel, N., Arteaga, A., Bustamante, L., Pichardo, F., Coloma, L. A., … Prost, S. (2018). Real-time DNA barcoding in a rainforest using nanopore sequencing:

579 opportunities for rapid biodiversity assessments and local capacity building. *GigaScience*,
580 *7*(4). doi:10.1093/gigascience/giy033
581 Quach, N., Goodman, M. F., & Shibata, D. (2004). In vitro mutation artifacts after formalin
582 fixation and error prone translesion synthesis during PCR. *BMC Clinical Pathology*, *4*, 1.
583 doi:10.1186/1472-6890-4-1
584 Rådström, P., Knutsson, R., Wolffs, P., Lövenklev, M., & Löfström, C. (2004). Pre-PCR
585 processing. *Molecular Biotechnology*, *26*(2), 133–146. doi:10.1385/MB:26:2:133
586 Sahlin, K., & Medvedev, P. (2018). De novo clustering of long-read transcriptome data using a
587 greedy, quality-value based algorithm. *BioRxiv*, 463463. doi:10.1101/463463
588 Schlaberg, R., Chiu, C. Y., Miller, S., Procop, G. W., & Weinstock, G. (2017). Validation of
589 Metagenomic Next-Generation Sequencing Tests for Universal Pathogen Detection.
590 *Archives of Pathology & Laboratory Medicine*, *141*(6), 776–786. doi:10.5858/arpa.2016-
591 0539-RA
592 Seimon, T. A., Ayebare, S., Sekisambu, R., Muhindo, E., Mitamba, G., Greenbaum, E., …
593 Plumptre, A. J. (2015). Assessing the Threat of Amphibian Chytrid Fungus in the
594 Albertine Rift: Past, Present and Future. *PLOS ONE*, *10*(12), e0145841.
595 doi:10.1371/journal.pone.0145841
596 Sepulveda, A., Hutchins, P., Massengill, R., & Dunker, K. (2018). Tradeoffs of a portable, field-
597 based environmental DNA platform for detecting invasive northern pike (Esox lucius) in
598 Alaska. *Management of Biological Invasions*, *9*(3), 253–258.
599 doi:10.3391/mbi.2018.9.3.07

Singh, U. A., Kumari, M., & Iyengar, S. (2018). Method for improving the quality of genomic DNA obtained from minute quantities of tissue and blood samples using Chelex 100 resin. In *Biological Procedures Online*. doi:10.1186/s12575-018-0077-6

Srinivasan, M., Sedmak, D., & Jewell, S. (2002). Effect of Fixatives and Tissue Processing on the Content and Integrity of Nucleic Acids. *The American Journal of Pathology*, *161*(6), 1961–1971. doi:10.1016/S0002-9440(10)64472-0

Srivathsan, A., Baloğlu, B., Wang, W., Tan, W. X., Bertrand, D., Ng, A. H. Q., … Meier, R. (2018). A MinION™-based pipeline for fast and cost-effective DNA barcoding. *Molecular Ecology Resources*, *18*(5), 1035–1049. doi:10.1111/1755-0998.12890

Srivathsan, A., Hartop, E., Puniamoorthy, J., Lee, W. T., Kutty, S. N., Kurina, O., & Meier, R. (2019). Rapid, large-scale species discovery in hyperdiverse taxa using 1D MinION sequencing. *BMC Biology*, *17*(1), 96. doi:10.1186/s12915-019-0706-9

Thomas, A. C., Tank, S., Nguyen, P. L., Ponce, J., Sinnesael, M., & Goldberg, C. S. (2019). A system for rapid eDNA detection of aquatic invasive species. *Environmental DNA*, edn3.25. doi:10.1002/edn3.25

Valentini, A., Pompanon, F., & Taberlet, P. (2009). DNA barcoding for ecologists. *Trends in Ecology & Evolution*, *24*(2), 110–117. doi:10.1016/j.tree.2008.09.011

Verma, S. K., & Singh, L. (2003). Novel universal primers establish identity of an enormous number of animal species for forensic application. *Molecular Ecology Notes*, *3*(1), 28–31. doi:10.1046/j.1471-8286.2003.00340.x

Waits, L. P., & Paetkau, D. (2005). Noninvasive Genetic Sampling Tools for Wildlife Biologists: A Review of Applications and Recommendations for Accurate Data Collection. *The*

*Journal of Wildlife Management*, *69*(4), 1419–1433. doi:10.2193/0022-541X(2005)69[1419:NGSTFW]2.0.CO;2

Walsh, P. S., Metzger, D. A., & Higuchi, R. (1991). Chelex 100 as a medium for simple extraction of DNA for PCR-based typing from forensic material. *BioTechniques*, *10*(4), 506–513.

628 **Figure 1:** Lab and SAIGA bioinformatics pipeline flowchart. Bioinformatics software and

629 parameters are indicated at each step.

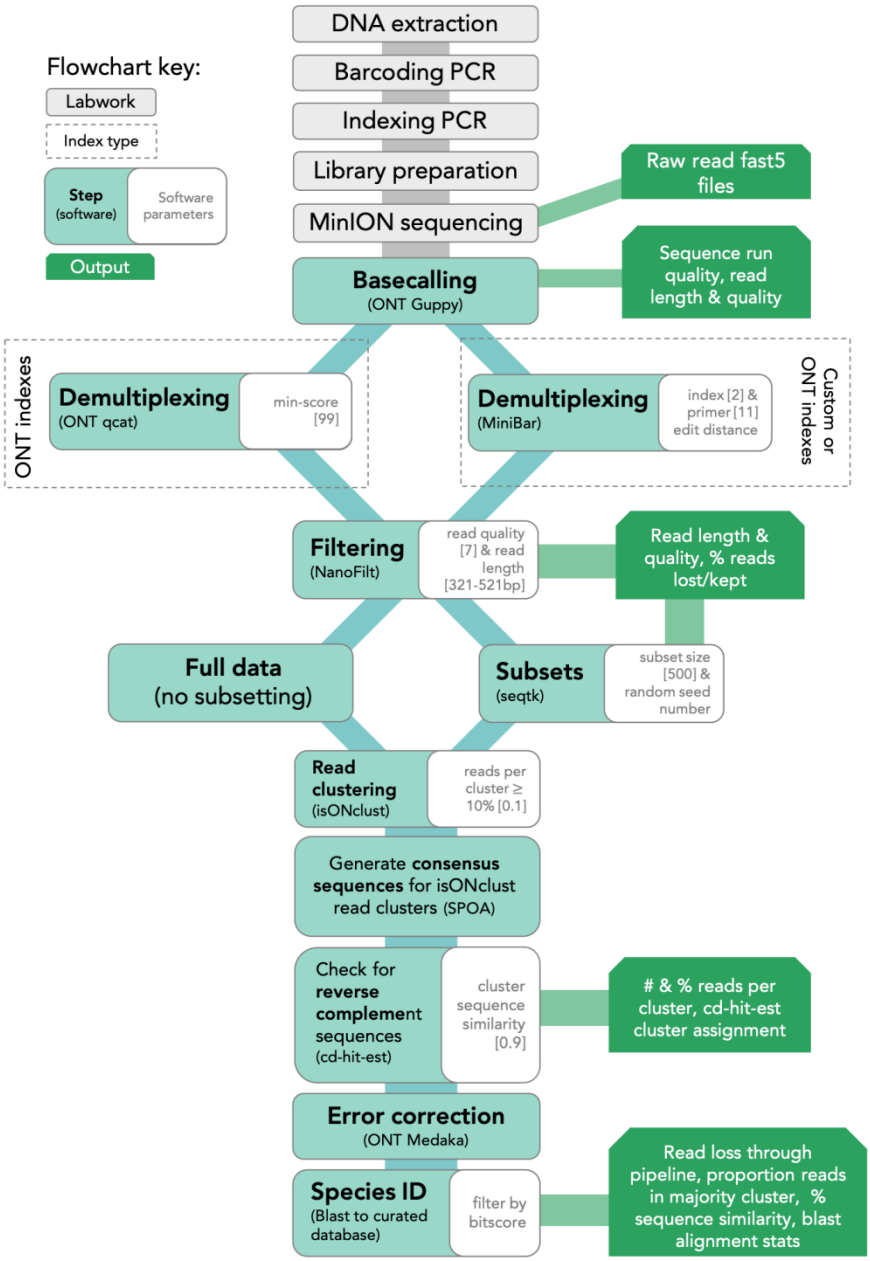


630

631

632 **Figure 2:** The number of reads assigned to each ONT index (01-12) per flow cell by MiniBar
633 and by qcat. For flow cell FAL19910, the 1st sequencing run used indexes 01-04 and the 2nd run
634 used indexes 05-10. For flow cell FAL19272, the 1st sequence run used indexes 01-06 and the
635 2nd run used indexes 07-12.

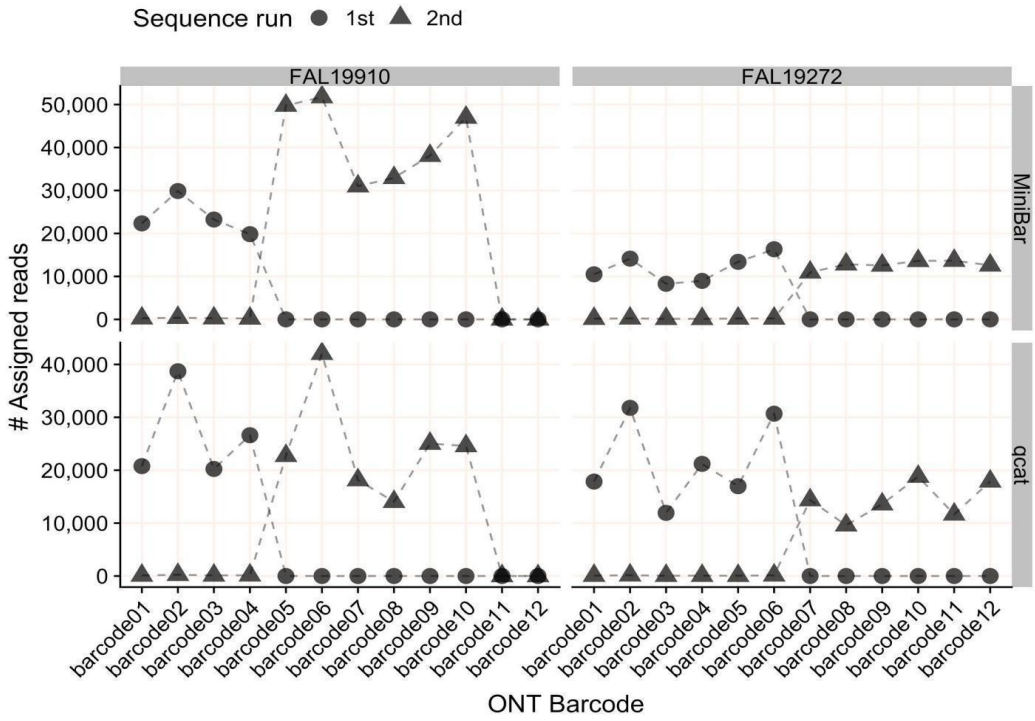


636

637

638

639 **Figure 3:** The percent of demultiplexed reads used to generate the final consensus sequence for
640 100R, 500R, and 5KR subsets for each species. Samples are labeled by tissue type and extraction
641 method (b=biomeme, c=chelex, q=qiagen). Points are linked by a grey line to show difference in
642 values from demultiplexers. Overlapping areas in orange indicate similar results for Minibar and
643 qcat analyses. Vertical dashed lines indicate samples with cinnamon teal contamination.

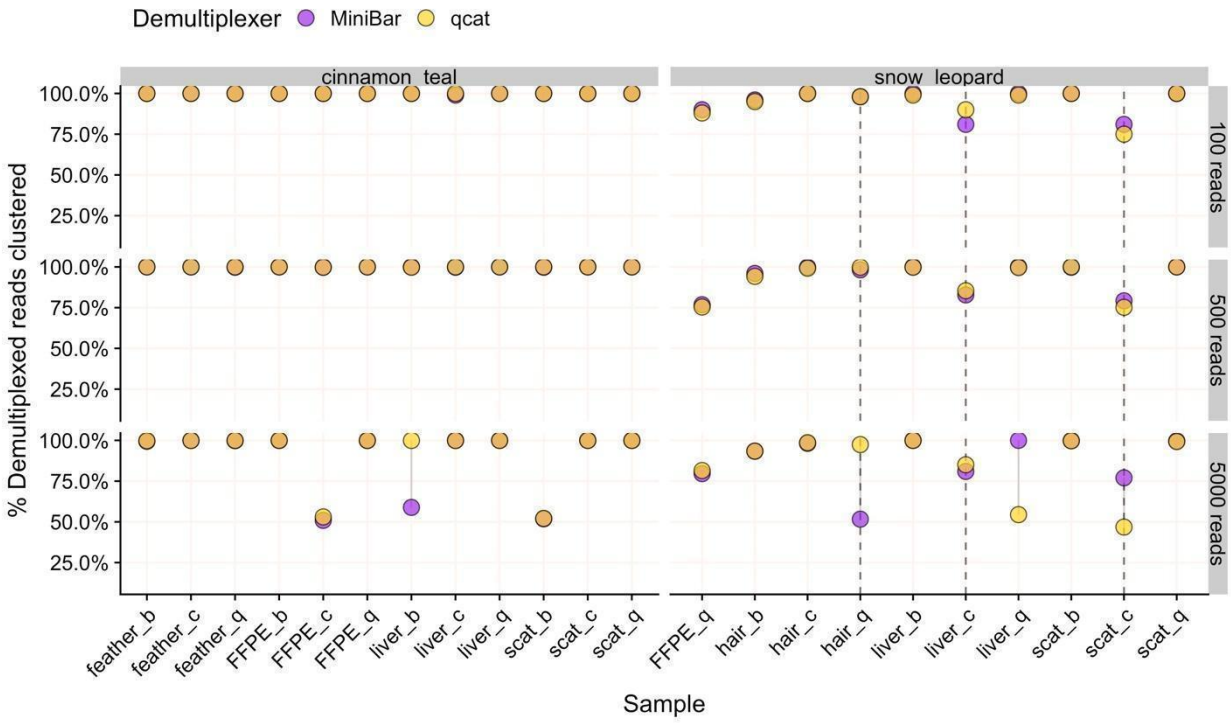


644

645

646 **Figure 4:** The percent sequence similarity of MinION consensus to Sanger sequence from Blast
647 for 100R, 500R, and 5KR subsets for each species. Samples are labeled by tissue type and
648 extraction method (b=biomeme, c=chelex, q=qiagen). Points are linked by a grey line to show
649 difference in values from demultiplexers. Overlapping areas in orange indicate similar results for
650 Minibar and qcat analyses. The horizontal dashed line is the 99% threshold for sequence
651 similarity. Vertical dashed lines indicate samples with cinnamon teal read contamination.

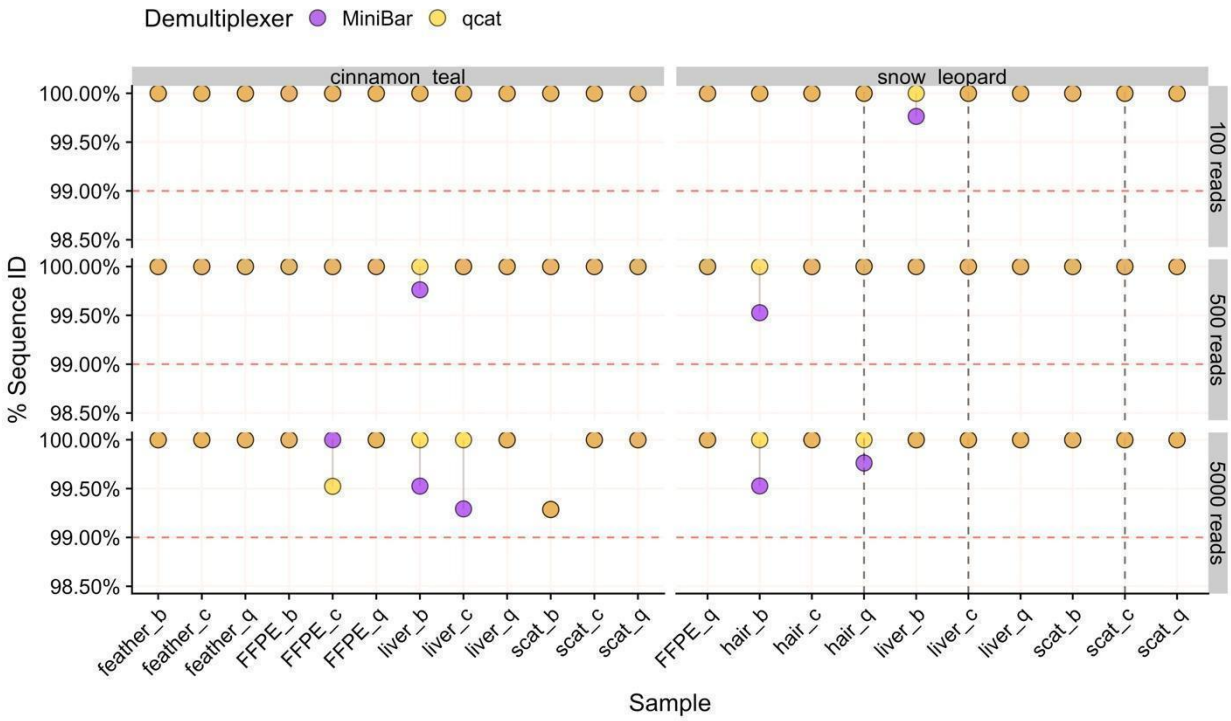


652

**Figure 5:** Screenshots of selected sections of the Mafft alignments for A) snow leopard and B) cinnamon teal showing nucleotide sites with differences between sequences in homopolymeric regions. Sanger sequences are listed above the black line and MinION consensus sequences below.

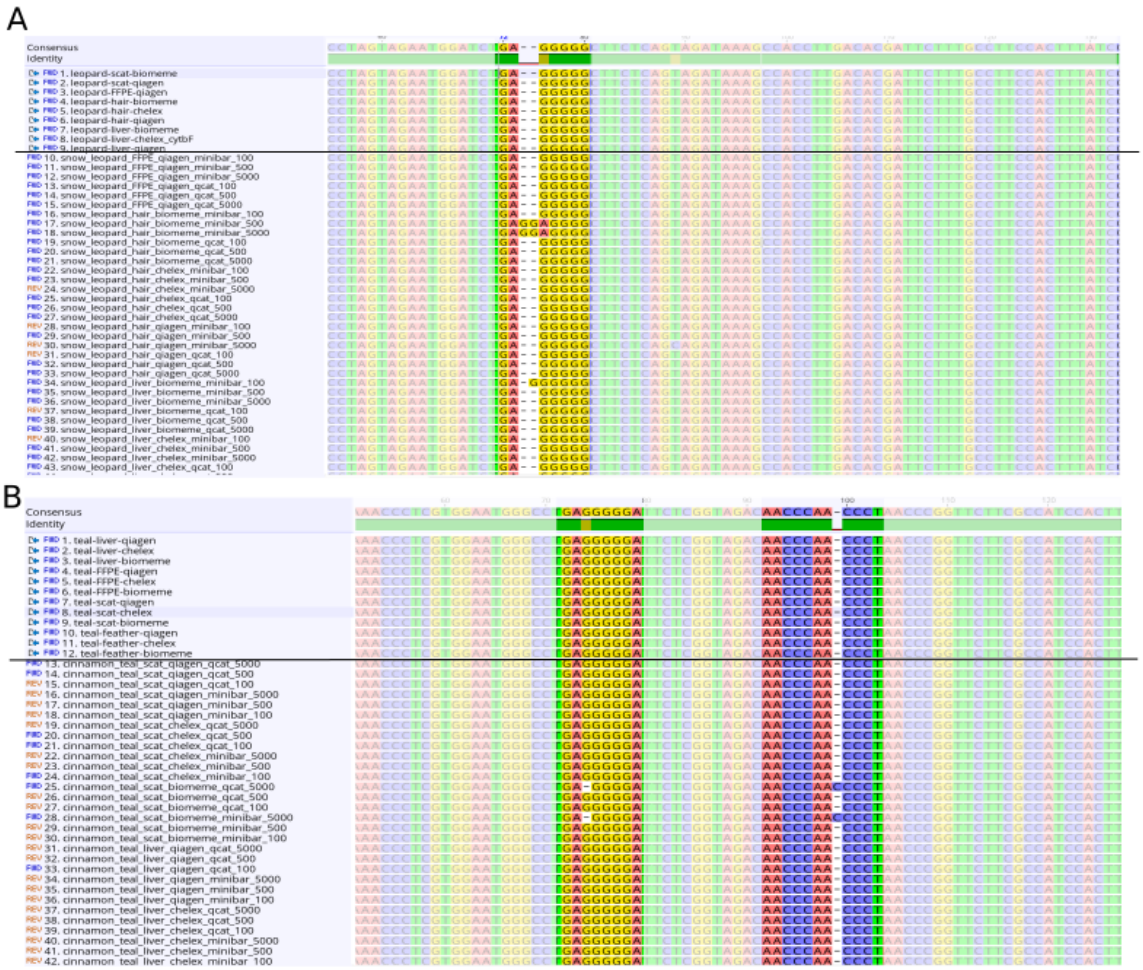

660 **Table 1:** Average and standard deviation (sd) for percent sequence similarity to Sanger

661 sequence, length of matching nucleotides, and number and percent of demultiplexed reads used

662 for the final consensus sequence from 100R, 500R, or 5KR read subsets demultiplexed with

663 MiniBar or qcat. Statistics were calculated across all tissue types and extraction method samples.

| **Subset** | **Demultiplexer** | **Average % ID (sd)** | **Average alignment length (bp) (sd)** | **Average number of clustered reads (sd)** | **Average % clustered reads (sd)** |
|---|---|---|---|---|---|
| 100 reads per sample (100R) | MiniBar | 99.99 (0.05) | 421.05 (0.21) | 97.5 (5.8) | 97.50% (0.06) |
| | qcat | 100 (0.00) | 420.5 (0.86) | 97.45 (6.01) | 97.45% (0.06) |
| 500 reads per sample (500R) | MiniBar | 99.97 (0.11) | 421.09 (0.43) | 484.5 (35.77) | 96.90% (0.07) |
| | qcat | 100 (0.00) | 420.82 (0.59) | 483.68 (38.32) | 96.73% (0.08) |
| 5,000 reads per sample (5KR) | MiniBar | 99.88 (0.24) | 421.18 (0.8) | 4411.14 (916.69) | 88.22% (0.18) |
| | qcat | 99.95 (0.18) | 420.41 (0.85) | 4456.14 (939.87) | 89.12% (0.19) |

664

665